



### Science Arts & Métiers (SAM)

is an open access repository that collects the work of Arts et Métiers Institute of Technology researchers and makes it freely available over the web where possible.

This is an author-deposited version published in: <https://sam.ensam.eu>  
Handle ID: <http://hdl.handle.net/10985/12997>

#### To cite this version :

Antoine PIERQUIN, Thomas HENNERON, Stephane CLENET - Data-Driven Model Order Reduction for Magnetostatic Problem Coupled with Circuit Equations - IEEE Transactions on Magnetics - Vol. 54, n°3, p.1-4 - 2018

Any correspondence concerning this service should be sent to the repository

Administrator : [scienceouverte@ensam.eu](mailto:scienceouverte@ensam.eu)



# Data-Driven Model Order Reduction for Magnetostatic Problem Coupled with Circuit Equations

A. Pierquin<sup>1</sup>, T. Henneron<sup>1</sup>, and S. Clénet<sup>1,2</sup>,

<sup>1</sup> Univ. Lille, EA 2697-L2EP-Laboratoire d'Electrotechnique et d'Electronique de Puissance, F-59000 Lille, France

<sup>2</sup>Arts et Métiers Paris Tech, F-59000 Lille, France

Among the model order reduction techniques, the Proper Orthogonal Decomposition (POD) has shown its efficiency to solve magnetostatic and magneto-quasistatic problems in the time domain. However, the POD is intrusive in the sense that it requires the extraction of the matrix system of the full model to build the reduced model. To avoid this extraction, nonintrusive approaches like the Data Driven (DD) methods enable to approximate the reduced model without the access to the full matrix system. In this article, the DD-POD method is applied to build a low dimensional system to solve a magnetostatic problem coupled with electric circuit equations.

*Index Terms*—Data driven, finite element model, model order reduction.

## I. INTRODUCTION

FINITE element method is often used to solve Maxwell's equations in electrical engineering. Unfortunately, in the case of a dynamic model, a fine spatial mesh and a large number of time steps induce high simulation duration. To reduce the computational time of large-scale dynamical Finite Element (FE) systems, Model Order Reduction (MOR) methods have been developed and studied in the literature. These methods consist in searching an approximation of the solution onto a subspace of the full solution space. Then, if the dimension of the subspace is low, the size of the equation system to solve can be highly reduced, as well as the simulation duration. One of the most popular MOR technique is the Proper Orthogonal Decomposition (POD) [1]. This approach requires to solve the full system for different time steps (called snapshots) to determine a reduced basis. Then, from the matrix system of the full model, the reduced model can be constructed and solved for all other time steps. This approach is well adapted if the matrix system can be extracted from the FE software. With commercial FE softwares, the matrix system is not necessarily accessible. As alternative, nonintrusive approaches of MOR, like Data Driven (DD) methods, have been developed in the literature [2]. One of these approaches (DD-POD) [3], builds an approximation of the reduced model from the known inputs and outputs of the full model. In low frequency, a significant number of magnetostatic or magnetodynamic problems have been studied with POD [4], [5], [6], [7] but not with nonintrusive approaches.

In this article, the DD-POD approach is applied to build a reduced model in order to solve a magnetostatic problem coupled with electric circuit equations using the vector potential formulation. The DD-POD reduced model is generated from the known inputs (voltage, current, resistances, ...) and the outputs (linkage flux, solution vector, ...) of the system.

In the first section of this article, the magnetostatic model and the electrical equations are introduced. In the second

one, the POD and the DD-POD are developed. Finally, an application example is studied in the last section: a three phase transformer is simulated with the POD method and the DD-POD approach. The results obtained with both reduced models are compared in terms of accuracy and computational time with the full model.

## II. MAGNETOSTATIC PROBLEM WITH ELECTRIC EQUATIONS

To solve a magnetostatic problem with  $N_{\text{ind}}$  stranded inductors coupled with electric circuit equations, the vector potential formulation can be used. In this case, as the magnetic flux density  $B$  is divergence-free ( $\nabla \cdot B = 0$ ), the magnetic flux density derives from a potential  $A$  such that  $B = \nabla \times A$ .

Using the magnetic behaviour law  $H = \nu B$ , with  $\nu$  the magnetic reluctivity, the expression of  $B$  is introduced into the Ampère's law  $\nabla \times H = J$ , to obtain the strong formulation

$$\nabla \times (\nu \nabla \times A) = J,$$

with  $H$  the magnetic field and  $J$  the source current density flowing through the inductors. The circuit equations linking the linkage flux  $\phi$ , the resistance  $R$ , the current  $i$  and the voltage  $v$  for each inductor  $k$  are added to the magnetostatic problem:

$$\frac{d\phi_k}{dt} + R_k i_k = v_k, \quad k = 1, \dots, N_{\text{ind}}.$$

Finally, discretizing the previous formulation using the FE method leads to the following system equations

$$\begin{bmatrix} 0 & 0 \\ F^T & 0 \end{bmatrix} \begin{bmatrix} \mathbf{a} \\ \mathbf{i} \end{bmatrix} + \begin{bmatrix} M & F \\ 0 & R \end{bmatrix} \begin{bmatrix} \mathbf{a} \\ \mathbf{i} \end{bmatrix} = \begin{bmatrix} 0 \\ \mathbf{v} \end{bmatrix}, \quad (1)$$

with  $\mathbf{a}$  the vector of size  $N_x$  composed of the circulations of the vector potential  $A$  along the edges of the mesh,  $\mathbf{i}$  the currents vector of the stranded inductors of size  $N_{\text{ind}}$ ,  $M$  the  $N_x \times N_x$  stiffness matrix depending on the magnetic reluctivity,  $F$  a  $N_x \times N_{\text{ind}}$  matrix depending on the geometries of the stranded inductors,  $\mathbf{v}$  the vector of the  $N_{\text{ind}}$  voltages applied to

the stranded inductor terminals and  $R$  the  $N_{\text{ind}} \times N_{\text{ind}}$  diagonal matrix of the winding resistances. The operator  $\cdot^T$  represents the transpose operator. The linkage flux  $\phi_k$  associated with the  $k$ -th inductor is expressed by  $\phi_k = \mathbf{f}_k^T \mathbf{a}$ , where  $\mathbf{f}_k$  is the  $k$ -th column of matrix  $F$ .

### III. MODEL ORDER REDUCTION

#### A. Proper Orthogonal Decomposition

Model order reduction can be performed using various methods. Among these methods, the POD is one of the most known and is applied to our problem. In order to conserve the structure of the matrix system during the reduction and to insure the stability, a structure preserving MOR [6] is performed: only the magnetic part of the problem is reduced. Then,  $\mathbf{a}$  is approximated by means of a reduced basis  $\Psi$  such that  $\mathbf{a} \simeq \Psi \mathbf{a}_r$ , where the size of  $\mathbf{a}_r$  is much smaller than this of  $\mathbf{a}$ . To define the matrix  $\Psi$ , the snapshot approach is used. The full model (1) is solved for different time steps and/or configurations in order to obtain a set of  $N_s$  solutions and to create the snapshot matrix  $X_s$  such as  $X_s = [\mathbf{a}(t_1), \mathbf{a}(t_2), \dots, \mathbf{a}(t_{N_s})] \in \mathbf{R}^{N_x \times N_s}$ . The snapshots can be determined during the first time steps or in a preprocessing step (greedy algorithm, typical tests, ...). The singular value decomposition applied to  $X_s$ , such as

$$X_s = U \Sigma W^T,$$

allows to obtain the reduced basis  $\Psi \in \mathbf{R}^{N_x \times N_r}$  formed by the  $N_r$  ( $N_r \leq N_s$ ) first columns of  $U$  which is an orthonormal matrix. The size  $N_r$  can be determined by a truncation strategy based on the analysis of the singular values. The reduced model of the magnetic equation in (1) (i.e.  $M\mathbf{a} + F\mathbf{i} = 0$ ) is obtained by replacing  $\mathbf{a}$  by  $\Psi \mathbf{a}_r$  and by performing a Galerkin projection. Finally, the POD model with structure preserving is defined by

$$\begin{bmatrix} 0 & 0 \\ F_r^T & 0 \end{bmatrix} \begin{bmatrix} \dot{\mathbf{a}}_r \\ \mathbf{i} \end{bmatrix} + \begin{bmatrix} M_r & F_r \\ 0 & R \end{bmatrix} \begin{bmatrix} \mathbf{a}_r \\ \mathbf{i} \end{bmatrix} = \begin{bmatrix} 0 \\ \mathbf{v} \end{bmatrix} \quad (2)$$

with  $F_r = \Psi^T F \in \mathbf{R}^{N_r \times N_{\text{ind}}}$  and  $M_r = \Psi^T M \Psi \in \mathbf{R}^{N_r \times N_r}$ .

The obtained system is solved by applying a time stepping scheme to simulate the problem on a given time interval. For each time step, it is always possible to go back to the full space of the solution by multiplying the reduced solution  $\mathbf{a}_r$  by the matrix  $\Psi$  in order to study the distribution of fields like the magnetic flux density. Left part of figure 1 presents the principle of the POD approach which involves to extract the matrices  $M$  and  $F$  of the FE software to build the reduced model.

#### B. Data-Driven POD

The principle of the DD approach combined with the POD method is to create an approximation of the reduced system (2) from the snapshots of the full model, without extracting the full matrix system (i.e. the matrices  $M$  and  $F$ ). Then, snapshot matrices associated with each output are defined such as

$$\begin{aligned} X_s &= [\mathbf{a}(t_1), \mathbf{a}(t_2), \dots, \mathbf{a}(t_{N_s})] \in \mathbf{R}^{N_x \times N_s}, \\ I_s &= [\mathbf{i}(t_1), \mathbf{i}(t_2), \dots, \mathbf{i}(t_{N_s})] \in \mathbf{R}^{N_{\text{ind}} \times N_s}, \end{aligned}$$

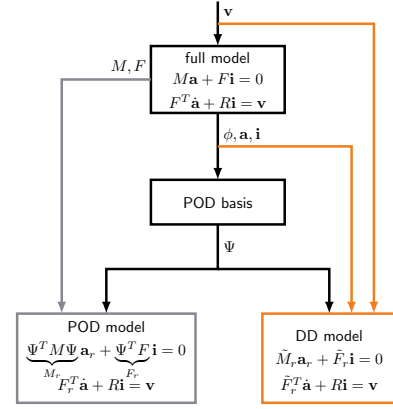


Fig. 1. Principle scheme of the POD and DD approaches.

$$\Phi_s = [\phi(t_1), \phi(t_2), \dots, \phi(t_{N_s})] \in \mathbf{R}^{N_{\text{ind}} \times N_s}.$$

From  $X_s$ , a reduced basis  $\Psi$  is determined in the same way as the one used for the POD (see III-A), and the snapshot matrix is projected onto the reduced space by  $X_r = \Psi^T X_s$ . The principle of the DD-POD is to find the reduced operators  $\tilde{F}_r \in \mathbf{R}^{N_r \times N_{\text{ind}}}$  and  $\tilde{M}_r \in \mathbf{R}^{N_r \times N_r}$ , approximations of  $F_r$  and  $M_r$  of the system (2), from  $I_s$ ,  $\Phi_s$  and  $X_r$ . Firstly, the operator  $\tilde{F}_r$  is deduced by using the relation between the solutions and the fluxes that must be verified for each snapshot:

$$\tilde{F}_r^T \mathbf{a}(t_\ell) = \phi(t_\ell), \quad \ell = 1 \text{ to } N_s.$$

Then by applying the transpose operator and considering the matrix expressions of the snapshots, we have the relation  $X_r^T \tilde{F}_r = \Phi_s^T$ . Each column  $\tilde{\mathbf{f}}_r|_k$  of  $\tilde{F}_r$  can be identified by solving the minimisation problem

$$\tilde{\mathbf{f}}_r|_k = \arg \min_{\mathbf{y} \in \mathbf{R}^{N_r}} \sum_{\ell=1}^{N_s} \left( \mathbf{a}^T(t_\ell) \mathbf{y} - \phi_k(t_\ell) \right)^2, \quad (3)$$

$k = 1$  to  $N_{\text{ind}}$ , which is equivalent to

$$\tilde{\mathbf{f}}_r|_k = \arg \min_{\mathbf{y} \in \mathbf{R}^{N_r}} \left\| X_r^T \mathbf{y} - \Phi_s^T|_k \right\|_2^2, \quad (4)$$

where  $\Phi_s^T|_k$  represents the  $k$ -th column of  $\Phi_s^T$ . Secondly, the matrix  $\tilde{M}_r$  is deduced from the first equation of (2). This relation must be verified for each snapshot such that

$$\tilde{M}_r \mathbf{a}(t_\ell) + \tilde{F}_r \mathbf{i}(t_\ell) = 0, \quad \ell = 1 \text{ to } N_s,$$

which can be matrixially written  $X_r^T \tilde{M}_r^T + I_s^T \tilde{F}_r^T = 0$ . The  $k$ -th row  $\tilde{\mathbf{m}}_r|_k$  of  $\tilde{M}_r$  can be determined by

$$\tilde{\mathbf{m}}_r|_k = \arg \min_{\mathbf{y} \in \mathbf{R}^{N_r}} \sum_{\ell=1}^{N_s} \left( \mathbf{a}^T(t_\ell) \mathbf{y} + (\mathbf{i}^T(t_\ell) \tilde{F}_r^T)_k \right)^2, \quad (5)$$

$k = 1$  to  $N_r$ , equivalent to

$$\tilde{\mathbf{m}}_r|_k = \arg \min_{\mathbf{y} \in \mathbf{R}^{N_r}} \left\| X_r^T \mathbf{y} + I_s^T \tilde{F}_r^T|_k \right\|_2^2, \quad (6)$$

where  $I_s^T \tilde{F}_r^T|_k$  represents the  $k$ -th column of  $I_s^T \tilde{F}_r^T$ . The solution of such minimisation problem is usually done using the pseudo-inverse of the matrix  $X_r^T$  since it is a linear least-square problem with an overdetermined system. Indeed, the

number of snapshots  $N_s$  is greater than the size of the reduced basis  $N_r$ . Figure 1 presents the principle of the DD-POD approach compared to the POD approach.

#### IV. APPLICATION

In term of application, a linear 3D three-phase EI transformer is considered. Figure 2 presents the mesh of the transformer, where only one quarter of the transformer is modeled. The time interval of simulation is  $[0:0.2s]$  with 400 time steps. To build the reduced models for the POD and DD-POD approaches, an Offline/Online method is used. During the Offline step, the snapshots are extracted from the typical tests at no-load and in short-circuit [7] on the first period, with 40 time-steps. Then, the POD and DD-POD models are defined and used to study another operating points during the Online step, with a resistive load and a self connected to the secondary windings. The full system has 75584 spatial unknowns when both reduced models are reduced to only 5 unknowns in this case due to a star secondary winding.

The reduced matrices obtained by the identification process of the DD-POD match with the reduced matrices based on the full matrix with the POD. Problem (3)-(4) provides an accurate operator

$$100 \cdot \frac{\|F_r - \tilde{F}_r\|}{\|F_r\|} = 2.7 \times 10^{-9}.$$

Problem (5)-(6) supplies also a precise operator, but less accurate than the previous one:

$$100 \cdot \frac{\|M_r - \tilde{M}_r\|}{\|M_r\|} = 1.6 \times 10^{-3}.$$

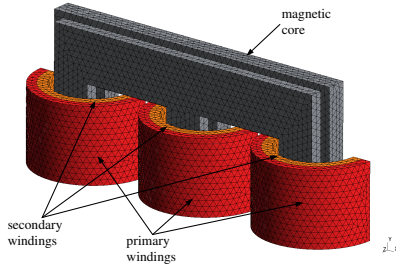
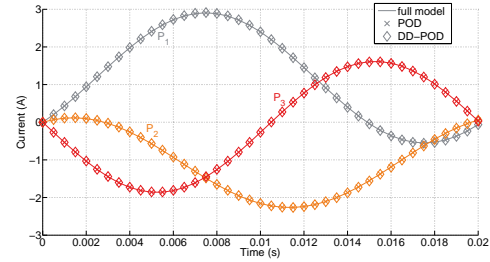


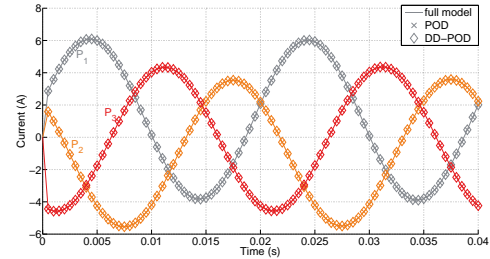
Fig. 2. Mesh of the 3D three-phase transformer.

Firstly, the reduced models are validated onto the no-load case. The evolutions of primary currents for the snapshots are presented on Fig. 3(a) for the full, POD and DD-POD models. Secondly, the current waveforms of the windings are compared in the case of a resistive load (Fig. 3(b)). Finally, the results are compared with the resistive and inductive loads. Figures 4(a) and 4(b) present the evolutions of the currents at the beginning of the simulation obtained from all models. In all cases, the waveforms of the currents from both reduced models are close to the references. Figures 5(a) and 5(b) present the evolutions of the error on the currents  $\mathbf{i}$  and on the solution vector  $\mathbf{a}$  versus the time. For each time step  $t_j$ , the error is given by the formula

$$\varepsilon_{\mathbf{y}}(t_j) = 100 \cdot \frac{\|\mathbf{y}_{\text{mor}}(t_j) - \mathbf{y}_{\text{ref}}(t_j)\|_2}{\|\mathbf{y}_{\text{ref}}(t_j)\|_2}.$$



(a) Primary currents at no-load



(b) Primary currents with a resistive load.

Fig. 3. Primary currents for the full, POD and DD-POD models at no-load and with a resistive load.

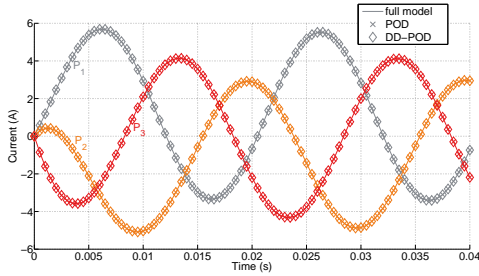
where  $\mathbf{y}$  is  $\mathbf{i}$  or  $\mathbf{a}$  and “mor” denotes the POD model or the DD-POD model. The error on the currents is always lower than 0.2% with the DD-POD model, whereas the error is less than 0.03% for the POD model. For the solution vector, the error is less than 0.02% with the DD-POD approach and 0.0025% with the POD method. The differences of error between the both reduced models are due to the approximations of the reduced operators in the case of the DD-POD approach. Nevertheless, the errors introduced by these approximations are low.

Figure 6 presents the distribution of the magnetic flux density from the full model at a given time step and the errors between the full model and the reduced models  $B_{\text{mor}} - B_{\text{ref}}$ . We can observe that the errors are smaller with the POD model than with the DD-POD model, nevertheless the magnitudes of the error of the DD-POD are small compared with the magnitude of the magnetic flux density. The maximal error is  $8.06 \times 10^{-7}$  and  $1.22 \times 10^{-4}$  for the POD and DD-POD models respectively.

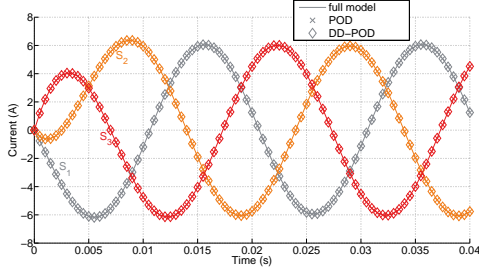
In term of computation time, the Offline phase requires 260s to extract the snapshots of the two typical tests. To build the reduced basis and then, the POD and DD-POD models, the running time is negligible (i.e. about 0.1s) compared with the offline step. For the solution of the problem on the time interval, the full model needs 1300 seconds and the reduced models require less than 0.1 second, leading to a speed-up of 20000.

#### V. CONCLUSION

In the context of MOR, the POD is often used. For dynamic cases, this method is robust, accurate and easy to be implemented. Nevertheless, it involves to have access to the matrices of the full system in order to build the reduced model. If the matrices are not available, it is possible to produce a

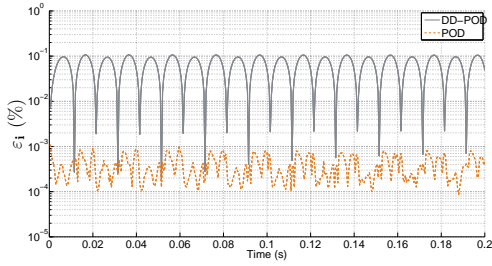


(a) Primary currents for the RL load.

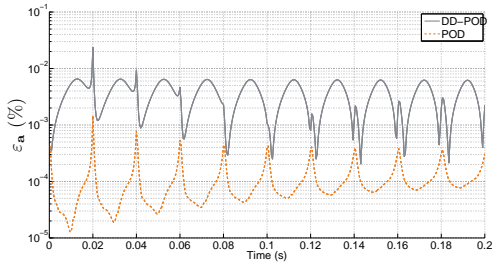


(b) Secondary currents for the RL load.

Fig. 4. Primary and secondary currents for the full, POD and DD-POD models with a RL load.



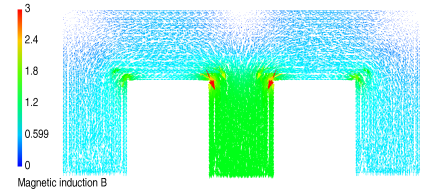
(a) Error on current for the RL load.



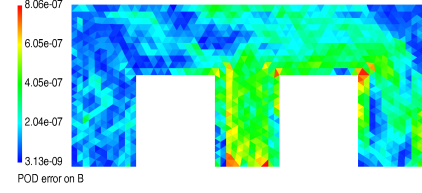
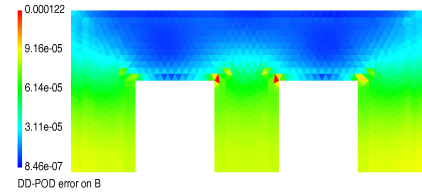
(b) Error on the solution vector for the RL load.

Fig. 5. Error on current and solution vector for the RL load.

reduced model only from inputs and outputs of the model by a data-driven technique. First, a reduced basis is calculated in the same way as classical POD. Secondly, the snapshots are projected onto the reduced space. After that, the process of the DD consists in determining the reduced matrices through a minimisation problem based on the fact that the matrices must verify the equations of the reduced system for each projected snapshot. By this way, a low dimensional system is determined without knowing the matrices of the full FE problem. From the application example, the results of the DD-POD model are less accurate than those from the POD model but the errors of the



(a) Distribution of the magnetic flux density (T) from the full model

(b)  $B_{pod} - B_{ref}$ (c)  $B_{dd-pod} - B_{ref}$ Fig. 6. Distribution of the magnetic flux density (T) from the full model (a) and of the error for the POD (b) and DD-POD (c) models ( $B_{mor} - B_{ref}$ ).

DD-POD are very small. Then, the DD-POD gives excellent accuracy in term of global and local solutions.

## REFERENCES

- [1] P. Holmes, J.L. Lumley and G. Berkooz, "Turbulence, Coherent Structures, Dynamical Systems and Symmetry", Cambridge, U.K.: Cambridge Univ. Press, 1996.
- [2] S. Ulaganathan, S. Koziel, A. Bekasiewicz, I. Couckuyt, E. Laermans and T. Dhaene, "Data-driven model based design and analysis of antenna structures", *IET Microwaves, Antennas & Propagation*, vol. 10, no. 13, pp. 1428-1434, Oct. 2016.
- [3] B. Peherstorfer and K. Willcox, "Data-driven operator inference for non-intrusive projection-based model reduction", *Computer Methods in Applied Mechanics and Engineering*, vol. 306, pp. 196-215, July 2016.
- [4] D. Schmidhäusler, S. Schöps and M. Clemens, "Reduction of Linear Subdomains for Non-Linear Electro-Quasistatic Field Simulations", *IEEE Transactions on Magnetics*, vol. 49, pp. 1669-1672, May 2013.
- [5] Y. Sato and H. Igarashi, "Model Reduction of Three-Dimensional Eddy Current Problems Based on the Method of Snapshots", *IEEE Transactions on Magnetics*, vol. 49, pp. 1697-1700, May 2013.
- [6] L. Montier, A. Pierquin, T. Henneron and S. Clénet, "Structure Preserving Model Reduction of Low Frequency Electromagnetic Problem based on POD and DEIM", *IEEE Transactions on Magnetics*, vol. 53, no. 6, June 2017.
- [7] T. Henneron and S. Clénet, "Model-Order Reduction of Multiple-Input Non-Linear Systems Based on POD and DEI Methods", *IEEE Transactions on Magnetics*, vol. 51, pp. 529-551, March 2015.